

Received April 11, 2020, accepted April 29, 2020, date of publication May 14, 2020, date of current version June 1, 2020.

Digital Object Identifier 10.1109/ACCESS.2020.2994361

Performance Analysis of Mixed Interference Aligned MIMO RF/Unified FSO DF Relaying With Heterodyne Detection and Two IMDD Models

OMER MAHMOUD SALIH AL-EBRAHEEMY¹, ANAS M. SALHAB¹, (Senior Member, IEEE),
MOHAMMED EL-ABSI², SALAM A. ZUMMO¹, (Senior Member, IEEE), AND
SALAMA S. IKKI³, (Senior Member, IEEE)

¹Electrical Engineering Department, King Fahd University of Petroleum and Minerals, Dhahran 31261, Saudi Arabia

²Digital Signal Processing Institute, University of Duisburg-Essen, 47057 Duisburg, Germany

³Electrical Engineering Department, Lakehead University, Thunder Bay, ON P7B 5E1, Canada

Corresponding author: Omer Mahmoud Salih Al-Ebraheemy (omermahmoud@gmail.com)

This work was supported by the Deanship of Scientific Research in King Fahd University of Petroleum and Minerals under Grant DF181024.

ABSTRACT This paper considers a dual-hop decode-and-forward (DF) mixed radio frequency (RF)/free space optical (FSO) relaying scheme. In this scheme, the first hop is a multiple-input multiple-output (MIMO) RF interference channel (IC), while the second hop is an FSO channel in which heterodyne detection (HD) as well as intensity modulation-direct detection (IMDD) are considered in a unified analysis manner. It is assumed that the MIMO RF links follow Rayleigh fading, whilst the FSO link encounters Málaga (\mathcal{M}) fading with pointing errors. In this work, the Interference alignment (IA) technique is utilized in the MIMO RF IC hop to eliminate the interference, and hence this leads to enhance the multiplexing gain in this hop, and accordingly the overall system performance is improved. The design of the IA precoding matrix and receiving interference eliminating matrix is performed by using adapting orthogonalized minimum leakage (OR-ML) algorithm. For the considered scheme, exact closed-form expressions are derived for the outage probability and ergodic capacity, in these expressions the best-known FSO channel capacity results are utilized. Moreover, not only the IMDD input-independent AWGN but also the IMDD cost-dependent AWGN channel is analyzed in these investigations. In addition, the system performance is studied asymptotically at the high SNRs region, where the diversity order and coding gain analyses are illustrated. Further, we allocate simulation results that verify the deduced analytical and asymptotic expressions.

INDEX TERMS Mixed MIMO RF/FSO relaying, interference alignment, Málaga (\mathcal{M}) fading, heterodyne detection, HD, intensity modulation-direct detection, IMDD, decode-and-forward, DF.

I. INTRODUCTION

In addition to their high bandwidth, free space optical (FSO) communications have many other advantages in comparison to radio frequency (RF) ones. Some of these advantages are: they are license-free spectrum communications, quick and easy to be deployed, more secure, and less demanding in terms of power consumption, mass requirements, and electromagnetic interference isolation. For these reasons, FSO has been implemented in many applications such as:

The associate editor coordinating the review of this manuscript and approving it for publication was Dominik Strzalka¹.

radio astronomy, remote sensing, last mile access, back-haul for cellular networks, and several more [1], [2].

Due to these distinctive features of FSO communication, there has been a great deal of research in this area recently; see [1], [2] and the references therein. A major challenge in FSO communications is the nonapplicability of the pure FSO schemes in mobile cellular networks. This nonapplicability comes from the requirement of the FSO schemes for the line-of-sight (LOS) link which is usually not guaranteed in mobile cellular networks in the link between the mobile station and the base station [3]. Nevertheless, an efficient method to overcome this challenge is to use the mixed RF/FSO

relay networks. In these networks, the mobile users (sources) transmit their info to a base transceiver station (relay) by RF link in the first hop, whereas in the second hop this relay forwards the info to the backbone network (destination) by FSO connection. Another advantage of this mixed relaying scheme is that it saves economical resources. This is done by avoiding the unnecessary costly implementations of optical fibers, for example in the suburbs and downtown regions, and concurrently conserving the RF spectrum while supporting high information rates by employing the FSO transmission. Thus, the mixed RF/FSO relay networks have been given great research attention.

Specifically, in [4] analytic expressions were derived for bit error rate (BER), outage probability, and ergodic capacity of variable gain amplify-and-forward (AF) mixed RF/FSO dual-hop relaying. It was assumed there that the RF hop experiences Rayleigh fading and the FSO hop experiences Gamma-Gamma (GG) fading with pointing errors, also both heterodyne detection (HD) along with intensity modulation-direct detection (IMDD) were considered for FSO detection. The symbol error rate (SER) was studied also for AF fixed gain mixed shadowed-Rician/GG without pointing error in [5]. A similar relaying system to that in [5] was investigated in terms of its outage probability in [6], however for mixed Rayleigh/Málaga (\mathcal{M}) fading with pointing error. Another similar system to that in [4] was investigated in [7] but for AF fixed gain relay assuming the existence of direct source-to-destination link. In addition, similar schemes to the one in [7] were analyzed in [8], without the direct source-to-destination link, and in [9] but for Nakagami- m fading RF link. A related scheme to those ones was analyzed in [10] for variable and fixed gain AF mixed Nakagami- m /GG relay system. Additionally, multiusers (sources) mixed RF/FSO AF relaying schemes with opportunistic scheduling were inspected in [11], [12]. Moreover, the BER and outage probability were investigated for AF (variable and fixed gain) mixed RF/FSO system in [13] using Nakagami- m for the RF hop and double generalized Gamma fadings for the FSO hop, and considering co-channel interferences, pointing error, and the existence of the direct RF connection.

Nevertheless, a main problem noticed in the AF mixed RF/FSO relaying systems, as in [4]–[13], is that they do not fulfill the nonnegativity constraint in the FSO IMDD transmitted signal, even when the subcarrier intensity modulation (SIM) is adopted in them. Namely, in those AF systems the relay receives a bipolar unbounded signal, which can not become positive, for the purpose of IMDD transmission, by mere amplification and/or deploying a DC bias [14]. As a result, the mathematical model and the findings of the above AF researches do not provide the real performance of these AF mixed RF/FSO relaying in which IMDD is implemented. This nonnegativity of the IMDD transmitted signal can be attained by the decode-and-forward (DF) mixed RF/FSO relay systems as the one studied in [15]–[18]. Particularly, an outage performance analysis was presented in [16] for mixed MIMO-RF/FSO DF relay systems with underlay

cognitive radio scenarios considering orthogonal space-time block coding (OSTBC) and transmit antenna selection (TAS). In [17] the performance of a multiuser dual-hop mixed RF/FSO DF relaying was analyzed using the V-BLAST strategy, and assuming GG faded IMDD channel with pointing error. Alternatively, the work in [18] investigated the performance of DF relaying for mixed $\eta - \mu$ faded RF/GG faded FSO with pointing errors.

However, the problem in the work in [16]–[18] is that it was not based on a correct capacity result for the IMDD channel. Alternatively, it was based on Shannon's capacity formula for the well-known power-constrained AWGN channel [19] which is not applicable for IMDD schemes since it does not take into account the nonnegativity constraint of the transmitted signal in the IMDD. This problem was fixed in [20] where the performance of DF relaying was analyzed for mixed Nakagami- m/\mathcal{M} fading with pointing errors and considering HD and IMDD in a unified manner wherein the best known capacity results for the FSO IMDD channel [21]–[24] were used.

In spite of considering the interference in analyzing the mixed RF/FSO relaying (see [13], [25]), as per our knowledge, no work in the literature investigated the performance of dual-hop mixed interference aligned MIMO RF interference channel¹ (IC)/FSO DF relaying despite its worthy applications. Therefore, this encourages us to analyze the performance of such system in which both HD and IMDD are considered in the FSO link. In this work the interference alignment (IA) technique is utilized in the MIMO RF IC hop to eliminate the interference, and hence this leads to enhance the multiplexing gain (degrees-of-freedom (DoF)) in this hop [27], and as a result the overall system performance is improved. To this end, IA exploits the knowledge of the channel state information (CSI) of all transmission links to build (beamform) the transmitted signals in a way that the interference signals at any receiver overlie on the same subspace while the desired signal, at that receiver, remains separable at another orthogonal subspace [27]. Thereby, interference elimination is possible by projecting the total received signal, using interference elimination combining matrix, on the desired signal subspace (zero-forcing the interference).

An important application of this scheme is the one in which the first hop is a MIMO uplink IC where K multiantennas-equipped mobile users (MSs) communicate with their corresponding K multiantennas-equipped base transceiver stations (BTSs) via RF links, specially when those MSs are located at the coverage border of their neighboring BTSs. While in the second hop these BTSs are connected with the backbone network via FSO links.

In this study, we utilize, in the system outage and capacity analyses, an accurate approximation for the IMDD channel

¹The interference channel [26] is a communication network in which the transmission medium is shared by transmitter–receiver pairs, where each transmitter sends desired info only to its receiver while causing interference to the other receivers.

capacity drawn in [21]–[24]. This rigorous approximation is tight in high SNRs, and thus it can act as channel capacity at that region. So, our analysis offers a rigorous quantitative comparison between IMDD and HD performances, and hence assists the planners in choosing whether to use HD (better info rates) or IMDD (less costs/complexity).

Additionally, not only the IMDD input-independent AWGN but also the IMDD cost-dependent AWGN channel is analyzed in these investigations. The difference between those two IMDD channels resides in the variance of the AWGN which does not depend on the input signal in the first model, however in the second model it is proportionate to the cost (constraint) of the input signal (average optical power). It is important also to state that the input-independent AWGN IMDD channel model [21], [22] is only valid where the receiver noises are dominated by thermal noise, and this is the case in the receivers which employ PIN-photodiode or in case of low optical powers. On the other hand, the cost-dependent AWGN IMDD channel model [23], [24] is useful wherever the receiver noises are dominated by shot noise, and this is the case in the receivers which employ avalanche photodiode (APD) or in case of high optical power.

In doing this analysis, we assume that the FSO links follow Málaga (\mathcal{M}) fading with pointing errors, whilst the MIMO RF links follow Rayleigh fading. Note that the \mathcal{M} fading model, as shown in [30], is valid under the whole range of atmospheric turbulence scenarios and it gives a very accurate fit to the experimental data. Also, the \mathcal{M} fading contains most of the FSO fading models (comprising GG) as special cases. Consequently, our analysis can be viewed as a generic one from the point of view of the FSO fading models.

Moreover, the system performance is studied asymptotically at the high SNRs region, where the diversity order and coding gain analyses are illustrated. It is found that when the system is dominated by the RF hop, the diversity order equals the square of the number of the interference-eliminated RF info streams. Alternatively, when the system is dominated by the FSO hop, the diversity order depends on the parameters of the atmospheric turbulences and pointing errors.

The analysis in this paper is accomplished in a unified way for the FSO connection which merges HD, IMDD input-independent, and IMDD cost-dependent in a unified expression for each of the statistical characteristics and/or performance measures.

Notation: $\det(\mathbf{Q})$ represents the determinant of matrix \mathbf{Q} . $(\mathbf{Q})^H$ represents the conjugate transpose of matrix \mathbf{Q} . $\text{Tr}(\mathbf{Q})$ denotes the trace of matrix \mathbf{Q} and $\mathbf{I}_{d \times d}$ is the identity matrix of size $d \times d$. $\mathbb{E}\{\cdot\}$ is the expectation operator. $\Gamma(\cdot)$ is the Gamma function as defined in [33, Eq. (8.310)], and $G[\cdot]$ is the Meijer’s G-function as defined in [33, Eq. (9.301)]. $\text{Pr}[\cdot]$ denotes the probability operator.

The rest of this paper is organized as follows. Section II presents the system model. The system analyses are offered in Section III. Section IV carries out and discusses the numerical and simulation results. Those results validate the deduced

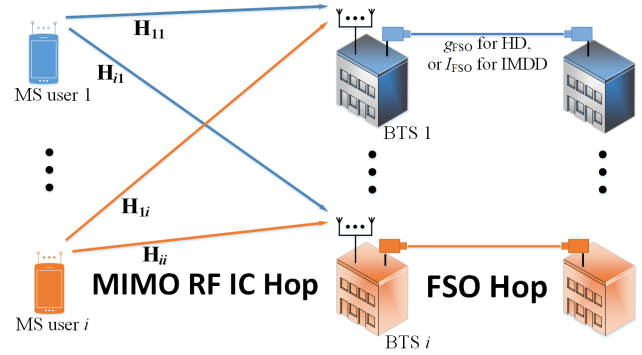


FIGURE 1. System model.

analytical and asymptotic expressions. Lastly, the conclusion is given in Section V.

II. SYSTEM AND CHANNEL MODELS

As shown in Fig. 1, the system under study is a dual-hop mixed MIMO RF IC/FSO DF relaying. In this system, K source-relay (transmitter-receiver) pairs form a MIMO RF interference channel in the first hop, where the transmitting MS user i (source i) has N_T antennas and needs to send d independent info streams, each one is equivalent to one DoF, to the receiving BTS i (relay i) which has N_R antennas. On the other hand, in the second hop the relays forward the sources messages to the corresponding destinations in the backbone network through FSO links.

A. THE MIMO RF IC HOP

In this work the IA technique is utilized in the MIMO RF IC hop to eliminate the interference, and hence results in enhancing the multiplexing gain (DoF) in this hop. The IA is feasible if there exist transmission precoding matrix $\mathbf{V}_i \in \mathbb{C}^{N_T \times d}$ at the transmitting MS user i (source i), and receiving interference elimination combining matrix $\mathbf{U}_i \in \mathbb{C}^{N_R \times d}$ at the receiving BTS i (relay i) with

$$\text{rank}(\mathbf{V}_i) = d, \quad \mathbf{V}_i^H \mathbf{V}_i = \mathbf{I}_{d \times d}, \quad (1)$$

$$\text{rank}(\mathbf{U}_i) = d, \quad \mathbf{U}_i^H \mathbf{U}_i = \mathbf{I}_{d \times d}, \quad (2)$$

such that [28]

$$\text{rank}(\mathbf{U}_i^H \mathbf{H}_{ij} \mathbf{V}_i) = d, \quad \forall i \in \{1, 2, \dots, K\}, \quad (3)$$

$$\mathbf{U}_i^H \mathbf{H}_{ij} \mathbf{V}_j = \mathbf{0}_{d \times d}, \quad \forall j \neq i, i, j \in \{1, 2, \dots, K\}, \quad (4)$$

where $\mathbf{H}_{ij} \in \mathbb{C}^{N_R \times N_T}$ is the matrix which represents the MIMO RF faded channel between relay i and source j . We assume that the elements of \mathbf{H}_{ij} are i.i.d. $\mathcal{CN}(0, \Omega_{\text{RF}})$, i.e., Rayleigh faded MIMO RF channel. Also, as mentioned in [28], the IA in $(N_R \times N_T, d)^K$ MIMO IC is feasible when

$$N_R + N_T - d(K + 1) \geq 0. \quad (5)$$

Assuming perfect CSI at each node, the interference eliminated received $d \times 1$ vector at the receiving BTS i is given

by

$$y_i = \sqrt{\frac{P_s}{d}} \mathbf{U}_i^H \mathbf{H}_{ii} \mathbf{V}_i x_i + \underbrace{\sum_{j=1, j \neq i}^K \sqrt{\frac{P_s}{d}} \mathbf{U}_i^H \mathbf{H}_{ij} \mathbf{V}_j x_j + \mathbf{U}_i^H n_i}_{\text{Zero due to(4)}} \quad (6)$$

$$= \sqrt{\frac{P_s}{d}} \tilde{\mathbf{H}}_{ii} x_i + \tilde{n}_i, \quad (7)$$

where x_i is the sent $d \times 1$ info vector from the transmitting MS user i , and $n_i \sim \mathcal{CN}(0, N_0 \mathbf{I})$ is the $N_R \times 1$ AWGN vector at the receiving BTS i , $\tilde{\mathbf{H}}_{ii} = \mathbf{U}_i^H \mathbf{H}_{ii} \mathbf{V}_i$, and $\tilde{n}_i = \mathbf{U}_i^H n_i$.

B. DESIGN OF THE PRECODING AND THE RECEIVING INTERFERENCE ELIMINATING MATRICES

The design of the b^{th} user precoding matrix \mathbf{V}_b and the interference suppression matrix \mathbf{U}_b associated to its corresponding b^{th} BTS is performed using adapting the orthogonalized minimum leakage (OR-ML) algorithm. In this algorithm, the interference I_b at each b^{th} BTS is minimized at the forward direction, where the interference is written as

$$I_b = \text{Tr}(\mathbf{U}_b^H \mathbf{Q}_b \mathbf{U}_b), \quad (8)$$

where \mathbf{Q}_b is the interference covariance matrix for that b^{th} BTS, and it is modeled as

$$\mathbf{Q}_b = \sum_{g=1, g \neq b}^K \frac{P_s}{d} \mathbf{H}_{bg} \mathbf{V}_g \mathbf{V}_g^H \mathbf{H}_{bg}^H. \quad (9)$$

To minimize the interference in this direction, \mathbf{U}_b is composed from the eigenvectors associated with the smallest eigenvalues of \mathbf{Q}_b .

In the reverse direction, the interference \hat{I}_k for the k^{th} user is minimized where

$$\hat{I}_k = \text{Tr}(\hat{\mathbf{U}}_k^H \hat{\mathbf{Q}}_k \hat{\mathbf{U}}_k), \quad (10)$$

and the reverse interference covariance matrix is

$$\hat{\mathbf{Q}}_k = \sum_{b=1, b \neq k}^K \frac{P_s}{d} \hat{\mathbf{H}}_{kb} \hat{\mathbf{V}}_b \hat{\mathbf{V}}_b^H \hat{\mathbf{H}}_{kb}^H, \quad (11)$$

where $\hat{\mathbf{H}}_{kb} = \mathbf{H}_{bk}^H$, $\hat{\mathbf{V}}_b = \mathbf{U}_b$ and $\hat{\mathbf{U}}_k = \mathbf{V}_k$. To minimize the interference in the reverse direction, $\hat{\mathbf{U}}_k$ (i.e. \mathbf{V}_k) is composed from the eigenvectors associated with the smallest eigenvalues of $\hat{\mathbf{Q}}_k$.

Since the design of the precoding and receiving interference elimination combining matrices iteratively can not remove the interference perfectly and completely, the interference term is still existed in the achievable data rate at each k^{th} user, R_k , which is given by

$$R_k = \frac{1}{2} \log_2 \det(\mathbf{I}_{d \times d} + \left(\frac{P_s}{d} \mathbf{U}_k^H \mathbf{H}_{kk} \mathbf{V}_k \mathbf{V}_k^H \mathbf{H}_{kk}^H \mathbf{U}_k\right) (\mathbf{U}_k^H \mathbf{Q}_k \mathbf{U}_k + N_0 \mathbf{I}_{d \times d})^{-1}). \quad (12)$$

Algorithm 1 Orthogonalized Minimum Leakage (OR-ML) Algorithm

- 1: **Start** with arbitrary $N_T \times d$ precoding matrices \mathbf{V}_k with $\mathbf{V}_k^H \mathbf{V}_k = \mathbf{I}_{d \times d} \quad \forall k \in \{1, \dots, K\}$.
- 2: **Repeat**
- 3: **Calculate** the interference covariance matrices $\mathbf{Q}_b \quad \forall b \in \{1, \dots, K\}$ according to (9).
- 4: **Compute** the interference suppression vector \mathbf{U}_b^{l*} for the l^{th} data stream at b^{th} BTS where $\mathbf{U}_b^{l*} = v_l[\mathbf{Q}_b] \quad \forall b \in \{1, \dots, K\}$, where $v_l[\mathbf{Q}_b]$ is the eigenvector of the l^{th} smallest eigenvalue of \mathbf{Q}_b .
- 5: **Combine** the interference suppression vectors \mathbf{U}_b^{l*} to form the interference suppression matrix $\mathbf{U}_b \quad \forall b \in \{1, \dots, K\}$.
- 6: **Reverse** the direction and set the reverse precoding matrix as the interference suppression matrix $\hat{\mathbf{V}}_b = \mathbf{U}_b \quad \forall b \in \{1, \dots, K\}$.
- 7: **Calculate** the reverse interference covariance matrices $\hat{\mathbf{Q}}_k \quad \forall k \in \{1, \dots, K\}$ according to (11).
- 8: **Compute** the reverse interference suppression vector $\hat{\mathbf{U}}_k^{l*}$ for the l^{th} data stream at k^{th} user where $\hat{\mathbf{U}}_k^{l*} = v_l[\hat{\mathbf{Q}}_k] \quad \forall k \in \{1, \dots, K\}$.
- 9: **Combine** the interference suppression vectors $\hat{\mathbf{U}}_k^{l*}$ to form the reverse interference suppression matrix $\hat{\mathbf{U}}_k \quad \forall k \in \{1, \dots, K\}$.
- 10: **Reverse** the direction and set the precoding matrix as the reverse interference suppression matrix $\mathbf{V}_k = \hat{\mathbf{U}}_k \quad \forall k \in \{1, \dots, K\}$.
- 11: **Until** a pre-defined number of iterations.
- 12: **Output** $\mathbf{U}_b \quad \forall b \in \{1, \dots, K\}$ and $\mathbf{V}_k \quad \forall k \in \{1, \dots, K\}$.

Thus, the total conveyed data rate at the network, user-sum rate R_s , is

$$R_s = \sum_{k=1}^K R_k \quad (13)$$

C. THE FSO HOP

After receiving the signal, the relay (BTS) forwards a decoded version of it to the destination in the second phase of transmission. Let's use x_{HD} and x_{IMDD} to designate the transmitted signal from the relay for the case of HD and IMDD, with the constraints $\mathbb{E}\{|x_{HD}|^2\} = 1$ and $\mathbb{E}\{x_{IMDD}\} = 1$ respectively. It is worthy noticing that in the IMDD case the average power constraint is on the expected signal value and not on its expected square as the signal in the IMDD technique is an optical intensity. So, the received signal at the destination for the case of HD and IMDD can be, respectively, expressed by

$$y_{HD} = \sqrt{P_r} g_{FSO} x_{HD} + n_{HD}, \quad (14)$$

$$y_{IMDD} = P_r I_{FSO} x_{IMDD} + n_{IMDD}, \quad (15)$$

where P_r is the relay transmitted power, g_{FSO} and $I_{FSO} = |g_{FSO}|^2$ designate the fading in the received electric field and irradiance, respectively. This fading is a result of the

atmospheric turbulence and pointing error in the relay-destination channel. In (14), $n_{\text{HD}} \sim \mathcal{CN}(0, N_{\text{HD}})$ is a complex AWGN. Whilst in (15), n_{IMDD} is a real AWGN where $n_{\text{IMDD}} \sim \mathcal{N}(0, N_{\text{IMDD}})$ for the IMDD input-independent AWGN model, and $n_{\text{IMDD}} \sim \mathcal{N}(0, 2P_r I_{\text{FSO}} N_{\text{HD}} \mathbb{E}\{x_{\text{IMDD}}\})$ for the IMDD cost-dependent AWGN channel under the assumption of relatively high P_r in comparison with the thermal and/or background noises power. The reader is referred to [23], [24] for details of the HD and the two IMDDs and their noises. So the SNRs at the destination are given as follows for the HD, IMDD input-independent, and IMDD cost-dependent,

$$\gamma_{\text{HD}} = \frac{P_r I_{\text{FSO}}}{N_{\text{HD}}}, \quad \gamma_{\text{IMDD}_{\text{inp}}} = \frac{P_r^2 I_{\text{FSO}}^2}{N_{\text{IMDD}}}, \quad \gamma_{\text{IMDD}_{\text{cost}}} = \frac{P_r I_{\text{FSO}}}{2N_{\text{HD}}}. \quad (16)$$

In this study, it is assumed that the FSO connection encounters \mathcal{M} fading with pointing error. In the development of the \mathcal{M} fading channel [30], the received signal is assumed to be consisted of a LOS component (U_L), a component coupled to the LOS and scattered by eddies on the propagation axis (U_S^C), and a component scattered by off-axis eddies (U_S^G) that is statistically independent from U_L and U_S^C . Thus by assuming the \mathcal{M} fading with pointing mismatch in the FSO channel, the probability density functions (pdfs) of the prior mentioned SNRs in (16) is given in the following unified formula [14]

$$f_{\gamma_{\text{FSO}}}^{\mathcal{M}}(\gamma) = \frac{\zeta^2 A}{2^s \gamma} \sum_{m=1}^{\beta} b_m G_{1,3}^{3,0} \left[B \left(\frac{w\gamma}{\mu_s} \right)^{1/s} \middle| \zeta^2 + 1 \right], \quad (17)$$

where γ_{FSO} represents the unified SNR of the FSO channel, A and b_m are as in [14, Eq. (6)], α is positive parameter and it is related to the effective number of the large-scale cells of the scattering (fading) process, β is a natural number and it is related to the effective number of the small-scale cells of the fading process,² $B = \zeta^2 \alpha \beta (g + \Omega') / [(\zeta^2 + 1)(g\beta + \Omega')]$, $\Omega' = \Omega + 2b_0\rho + 2\sqrt{2b_0\rho\Omega} \cos(\Phi_A - \Phi_B)$ is the average power of the coherent contribution, $\Omega = \mathbb{E}\{|U_L|^2\}$, $\mathbb{E}\{|U_S^C|^2\} = 2b_0\rho$, Φ_A and Φ_B are deterministic phases of the LOS and the coupled-to-LOS signal components, respectively, $2b_0 = \mathbb{E}\{|U_S^C|^2 + |U_S^G|^2\}$ is the average power of all scattered components, $g = \mathbb{E}\{|U_S^G|^2\} = 2b_0(1 - \rho)$, the parameter $0 \leq \rho \leq 1$ denotes the part of the scattered power coupled to the LOS, ζ is the ratio between the equivalent beam radius and the standard deviation of the pointing error displacement at the receiver (i.e. $\zeta \rightarrow \infty$, indicates the nonpointing error case) [32], A_0 is a parameter that represents the pointing losses (or typically the FSO link losses), s and w are the parameters which determine the sort of the FSO detections, i.e., $(s, w) = (1, 1)$, $(2, 1)$ or $(1, 2)$ for the HD,

²The fading parameters α and β reflect the atmospheric turbulences condition (The Rytov variance) with low values basically denoting strong (severe) atmospheric turbulent situation [20].

IMDD input-independent, and IMDD cost-dependent respectively, and where $\mu_1 \triangleq P_r \mathbb{E}\{I_{\text{FSO}}\} / N_{\text{HD}} = A_0 P_r \zeta^2 (g + \Omega') / [(\zeta^2 + 1)N_{\text{HD}}]$,³ and for normalization purposes $\mu_2 \triangleq P_r^2 \mathbb{E}\{I_{\text{FSO}}^2\} / N_{\text{IMDD}}$ as defined previously in [14] and the references therein. This definition leads to $\mu_2 = A_0^2 P_r^2 \zeta^4 (g + \Omega')^2 / [(\zeta^2 + 1)^2 N_{\text{IMDD}}]$. From these expressions of μ_1 , μ_2 , and (16), it can be seen that μ_s is proportional to the average of the unified FSO SNR ($\bar{\gamma}_{\text{FSO}}$). To be exact, $\mu_1 = \bar{\gamma}_{\text{HD}} = 2\bar{\gamma}_{\text{IMDD}_{\text{cost}}}$; however $\mu_2 = \bar{\gamma}_{\text{IMDD}_{\text{inp}}} \frac{\mathbb{E}\{I_{\text{FSO}}^2\}}{\mathbb{E}\{I_{\text{FSO}}\}^2} = \frac{\zeta^2 (\zeta^2 + 1)^{-2} (\zeta^2 + 2)(g + \Omega')^2}{\alpha^{-1} (\alpha + 1) [2g(g + 2\Omega') + \Omega'^2 (1 + 1/\beta)]} \bar{\gamma}_{\text{IMDD}_{\text{inp}}}$.³

Note that having $\rho = 1$ (i.e. $g = 0$) results in $Ab_m = 2/(\Gamma(\alpha)\Gamma(\beta))$ when $m = \beta$ and $Ab_m = 0$ for all other m . So in this case, by having $\rho = 1$, and $\Omega' = 1$ (for normalization), the pdf $f_{\gamma_{\text{FSO}}}^{\mathcal{M}}(\gamma)$ in (17) turns into the special case of the GG distribution with pointing errors [31]. By having $\rho = 1$, the power $\mathbb{E}\{|U_S^G|^2\} \triangleq g = 0$, this means that the GG fading channel neglects the component of the received signal scattered by the off-axis eddies (U_S^G). Thus, by using $\Omega' = 1$ and $\rho = 1$ in (17), the pdf of the unified FSO SNR in the GG fading with pointings error can be presented by

$$f_{\gamma_{\text{FSO}}}^{\text{GG}}(\gamma) = \frac{\zeta^2}{s \gamma \Gamma(\alpha)\Gamma(\beta)} G_{1,3}^{3,0} \left[\frac{\zeta^2 \alpha \beta}{(\zeta^2 + 1)} \left(\frac{w\gamma}{\mu_s} \right)^{1/s} \middle| \zeta^2 + 1 \right]. \quad (18)$$

III. SYSTEM PERFORMANCE ANALYSIS

A. OUTAGE PROBABILITY

The outage probability (P_{out}) is a substantial performance indicator in slow fading channels.⁴ It can be presented, as in [34], by $P_{\text{out}} = \Pr[C < R]$, where R is the end to end (e2e) required information rate in bits/channel-use, C is a random variable and it is a function on the random e2e channel equivalent SNR. The realization of C designates the e2e channel capacity for a given realization of the e2e equivalent SNR of the channel. As in any DF dual-hop system, in the considered system, the outage event takes place whenever the first hop or the second hop falls in an outage. Thence, the P_{out} in the system under study can be expressed as⁵

$$P_{\text{out}} = \Pr \left[C_{\text{RF}} < 2R \cup C_{\text{FSO}} < 2R \right], \quad (19)$$

where C_{RF} and C_{FSO} are related to channel capacity of the first hop (RF hop) and second hop (FSO hop), respectively.

Particularly, C_{RF} is a random variable and its realization is the channel capacity of the RF hop given the related realization of the effective channel fading matrix (\tilde{H}_{ii}) of the first hop. However by utilizing the IA, the first hop is effectively a

³ $\mathbb{E}\{I_{\text{FSO}}\}$ and $\mathbb{E}\{I_{\text{FSO}}^2\}$ are derived from [31, Eq. (33)].

⁴Note that the channels in most of the RF and FSO schemes, including our system in this work, are slow fading channels [2], [34].

⁵Here the required data rates in the two hops are assumed to be identical, and thence the factor 2 results by assuming that the e2e transmission (from the source to destination) takes place on two equal phases (two equal channel uses). This lets each hop data rate to be twice the e2e data rate.

MIMO AWGN channel as represented by (7). Thus, by utilizing the MIMO AWGN channel capacity expression, as given in [34], we obtain⁶

$$C_{RF} = \log \left[\det \left(\frac{P_s}{N_o d} \tilde{H}_{ii} \tilde{H}_{ii}^H + I_{d \times d} \right) \right] \quad (20)$$

However, since the RF channel matrix has i.i.d. $\mathcal{CN}(0, \Omega_{RF})$ elements, then with probability 1 this matrix has full rank, and it is well-conditioned [34]. Due to these properties, we get $\tilde{H}_{ii} \tilde{H}_{ii}^H = \lambda_{hh} I_{d \times d}$. Furthermore, by using the eigenvalues identities, it can be shown that $\lambda_{hh} d = \text{Tr}(\tilde{H}_{ii} \tilde{H}_{ii}^H)$, and this means that $\tilde{H}_{ii} \tilde{H}_{ii}^H = \frac{\text{Tr}(\tilde{H}_{ii} \tilde{H}_{ii}^H)}{d} I_{d \times d}$. Then, employing the last expression of $\tilde{H}_{ii} \tilde{H}_{ii}^H$ in (20) leads to

$$C_{RF} = d \log \left(1 + \frac{P_s}{N_o d^2} \text{Tr}(\tilde{H}_{ii} \tilde{H}_{ii}^H) \right). \quad (21)$$

In a compact way, (21) can be written as

$$C_{RF} = d \log(1 + \gamma_{RF}), \quad (22)$$

where γ_{RF} is defined by $\gamma_{RF} = \frac{P_s}{N_o d^2} \text{Tr}(\tilde{H}_{ii} \tilde{H}_{ii}^H)$, and it is used to represent the effective SNR of the MIMO RF link (or in short we may call it the RF SNR). As a result of assuming i.i.d. $\mathcal{CN}(0, \Omega_{RF})$ elements of the RF channel matrix, γ_{RF} has a gamma pdf which is given by [35]

$$f_{\gamma_{RF}}(\gamma) = \left(\frac{d^2}{\bar{\gamma}_{RF}} \right)^{d^2} \frac{\gamma^{d^2-1}}{(d^2-1)!} \exp \left(-\frac{d^2}{\bar{\gamma}_{RF}} \gamma \right), \quad (23)$$

where $\bar{\gamma}_{RF}$ denotes the average effective SNR of the MIMO RF link (or shortly the average RF SNR). Namely, $\bar{\gamma}_{RF} = \mathbb{E}\{\gamma_{RF}\} = \frac{P_s}{N_o} \Omega_{RF}$.

On the other side, C_{FSO} is a function on the random SNR of the FSO hop, and thence it is a random variable. Additionally, in case of HD the realization of C_{FSO} designates the channel capacity of the second hop given the realization of the second hop SNR (γ_{HD}). Whereas, in case of IMDD we let the realization of C_{FSO} designates a precise approximation⁷ of the channel capacity of the second hop given the related realization of the second hop SNR ($\gamma_{IMDD_{indp}}$ or $\gamma_{IMDD_{cost}}$). But, given γ_{HD} , $\gamma_{IMDD_{indp}}$ or $\gamma_{IMDD_{cost}}$ the FSO hop is, respectively, an AWGN channel, IMDD input-independent AWGN channel, or IMDD cost-dependent AWGN channel as expressed by (14) or (15). So, by utilizing the expressions of the AWGN channel capacity [19] and the approximations of both IMDD AWGN channel capacities [21], [24] we get C_{FSO} in the following unified form

$$C_{FSO} = \log(1 + \gamma_{FSO}^{eff}), \quad (24)$$

where γ_{FSO}^{eff} is used to represent the unified effective SNR of the FSO channel, i.e., γ_{FSO}^{eff} equals either γ_{HD} , $\sqrt{\frac{e}{2\pi}} \gamma_{IMDD_{indp}}$, or $\sqrt{\frac{e}{2\pi}} \gamma_{IMDD_{cost}}$ based on the used FSO transmission type.

⁶Unless otherwise specified, in this work, the log base is 2.

⁷This approx. is used as the IMDD channel capacity is so far unknown [22]. Nonetheless, this approx. is very rigorous at high SNRs, and thus it can act as the IMDD channel capacity in that region.

Because it is important in what follows, let's derive the pdf of γ_{FSO}^{eff} . From $f_{\gamma_{FSO}^{eff}}^{\mathcal{M}}(\gamma)$ in (17), and by random variable transformation, the pdf of γ_{FSO}^{eff} can be expressed in a unified form as

$$f_{\gamma_{FSO}^{eff}}^{\mathcal{M}}(\gamma) = \frac{w \zeta^2 A}{2 \gamma} \sum_{m=1}^{\beta} b_m G_{1,3}^{3,0} \left[\frac{B(\gamma/c)^w}{\mu_s^{1/s}} \middle| \zeta^2 + 1, \zeta^2, \alpha, m \right], \quad (25)$$

where the constant $c = 1, \sqrt{\frac{e}{2\pi}}$, or $\sqrt{\frac{e}{4\pi}}$ for HD, IMDD input-independent, or IMDD cost-dependent, respectively, and the remainder of the parameters are as in (17). Note that using $\Omega' = 1$ and $\rho = 1$ in (25), results in the following pdf of γ_{FSO}^{eff} in the special case of GG fading with pointing errors

$$f_{\gamma_{FSO}^{eff}}^{GG}(\gamma) = \frac{w \zeta^2}{\gamma \Gamma(\alpha) \Gamma(\beta)} G_{1,3}^{3,0} \left[\frac{\zeta^2 \alpha \beta (\gamma/c)^w}{(\zeta^2 + 1) \mu_s^{1/s}} \middle| \zeta^2 + 1, \zeta^2, \alpha, \beta \right]. \quad (26)$$

Now with the help of (22) and (24), the P_{out} in (19) can be given by [36]

$$P_{out} = \Pr[\gamma_{RF} < (2^{2R/d} - 1)] + \Pr[\gamma_{FSO}^{eff} < (2^{2R} - 1)] - \Pr[\gamma_{RF} < (2^{2R/d} - 1)] \Pr[\gamma_{FSO}^{eff} < (2^{2R} - 1)]. \quad (27)$$

From (27) P_{out} can be expressed in terms of the cumulative distribution functions (CDFs) of γ_{RF} and γ_{FSO}^{eff} evaluated at $\gamma_{out1} \triangleq (2^{2R/d} - 1)$ and $\gamma_{out2} \triangleq (2^{2R} - 1)$, respectively. Consequently, we get

$$P_{out} = F_{\gamma_{RF}}(\gamma_{out1}) + F_{\gamma_{FSO}^{eff}}^{\mathcal{M}}(\gamma_{out2}) - F_{\gamma_{RF}}(\gamma_{out1}) F_{\gamma_{FSO}^{eff}}^{\mathcal{M}}(\gamma_{out2}), \quad (28)$$

where $F_{\gamma_{RF}}(\gamma)$ and $F_{\gamma_{FSO}^{eff}}^{\mathcal{M}}(\gamma)$ are the CDFs of γ_{RF} and γ_{FSO}^{eff} , respectively. Those CDFs are, respectively, expressed, after integrating their pdfs in (23) and (25) with respect to γ , as follows

$$F_{\gamma_{RF}}(\gamma) = 1 - \exp \left(-\frac{d^2 \gamma}{\bar{\gamma}_{RF}} \right) \sum_{i=0}^{d^2-1} \frac{1}{i!} \left(\frac{d^2 \gamma}{\bar{\gamma}_{RF}} \right)^i, \quad (29)$$

$$F_{\gamma_{FSO}^{eff}}^{\mathcal{M}}(\gamma) = \frac{\zeta^2 A}{2} \sum_{m=1}^{\beta} b_m G_{2,4}^{3,1} \left[\frac{B(\gamma/c)^w}{\mu_s^{1/s}} \middle| 1, \zeta^2 + 1, \zeta^2, \alpha, m, 0 \right]. \quad (30)$$

Then, by exploiting the CDFs (29) and (30) in (28) and after some algebraic simplifications, we get

$$P_{out} = 1 - \left(\exp \left(-\frac{d^2 \gamma_{out1}}{\bar{\gamma}_{RF}} \right) \sum_{i=0}^{d^2-1} \frac{1}{i!} \left(\frac{d^2 \gamma_{out1}}{\bar{\gamma}_{RF}} \right)^i \right) \times \left(1 - \frac{\zeta^2 A}{2} \sum_{m=1}^{\beta} b_m G_{2,4}^{3,1} \left[\frac{B(\gamma_{out2}/c)^w}{\mu_s^{1/s}} \middle| 1, \zeta^2 + 1, \zeta^2, \alpha, m, 0 \right] \right). \quad (31)$$

Recall that the P_{out} in (31) is in case of \mathcal{M} faded FSO hop. However, to have P_{out} in the special case of the GG faded FSO hop, the CDF $F_{\gamma_{FSO}^{eff}}^{\mathcal{M}}(\gamma)$ in (28) must be changed

by the CDF $F_{\gamma_{\text{FSO}}^{\text{eff}}}^{\text{GG}}(\gamma)$ that can be given, by integrating its corresponding pdf in (26), as follows

$$F_{\gamma_{\text{FSO}}^{\text{eff}}}^{\text{GG}}(\gamma) = \frac{\zeta^2}{\Gamma(\alpha)\Gamma(\beta)} G_{2,4}^{3,1} \left[\frac{\zeta^2 \alpha \beta (\gamma/c)^w}{(\zeta^2 + 1) \mu_s^{1/s}} \middle| \begin{matrix} 1, \zeta^2 + 1 \\ \zeta^2, \alpha, \beta, 0 \end{matrix} \right]. \quad (32)$$

B. ASYMPTOTIC OUTAGE PROBABILITY

The expression of the outage in (31) is complicated, and thus, from it, we can not easily see the effects of the system parameters on the system outage. So, in this section a simpler (asymptotic) expression is derived for the outage probability at the high SNRs. This asymptotic P_{out} helps more in analyzing and understanding the system performance by containing some outage performance indicators in its expression.

Particularly, at high SNRs, the asymptotic outage probability can be typically represented as $P_{\text{out}}^{(a)} \simeq (G_c \text{SNR})^{-G_d}$, where G_c and G_d are outage performance indicators that are, respectively, named the coding gain and diversity order associated with the P_{out} of the system [29]. The diversity order G_d identifies the slope of the P_{out} versus the average SNR log-log curve at high SNRs, whilst $\log G_c$ identifies the horizontal shift of this curve in comparison with a curve of benchmark outage probability given by $(\text{SNR})^{-G_d}$.

Therefore, to analyze G_d and G_c of our system, we should reduce (31) to the standard $P_{\text{out}}^{(a)}$ formula. For this purpose, we modify Eq. (28) as follows: firstly we change the used CDFs by their asymptotic versions on high SNRs, then we neglect the last term as it is ignorable on high SNRs. These modifications result in

$$P_{\text{out}}^{(a)} = F_{\gamma_{\text{RF}}}^{(a)}(\gamma_{\text{out1}}) + F_{\gamma_{\text{FSO}}^{\text{eff}}}^{\mathcal{M}(a)}(\gamma_{\text{out2}}), \quad (33)$$

where $F_{\gamma_{\text{RF}}}^{(a)}(\gamma_{\text{out1}})$ and $F_{\gamma_{\text{FSO}}^{\text{eff}}}^{\mathcal{M}(a)}(\gamma_{\text{out2}})$ are the asymptotic CDFs of γ_{RF} and $\gamma_{\text{FSO}}^{\text{eff}}$ at the high SNRs. Next, Let's determine those asymptotic CDFs. To obtain $F_{\gamma_{\text{RF}}}^{(a)}(\gamma)$ we begin by applying the high SNR limit ($\lim_{\bar{\gamma}_{\text{RF}} \rightarrow \infty} \exp(-\frac{d^2 \gamma}{\bar{\gamma}_{\text{RF}}}) = 1$) in (23) to attain $f_{\gamma_{\text{RF}}}^{(a)}(\gamma) = (\frac{d^2}{\bar{\gamma}_{\text{RF}}})^d \frac{\gamma^{d^2-1}}{(d^2-1)!}$, then by integrating this asymptotic pdf we get

$$F_{\gamma_{\text{RF}}}^{(a)}(\gamma) = \left(d^2 / \bar{\gamma}_{\text{RF}} \right)^d \gamma^{d^2} / (d^2)!. \quad (34)$$

Then again to derive $F_{\gamma_{\text{FSO}}^{\text{eff}}}^{\mathcal{M}(a)}(\gamma)$, we adjust (30) by using [37, Eq. (07.34.06.0006.01)]⁸ which is the Meijer G-function series representation for $\frac{1}{\mu_s} \rightarrow 0$, i.e.,⁸ $\bar{\gamma}_{\text{FSO}} \rightarrow \infty$ (on the high SNRs). By doing this we obtain

$$F_{\gamma_{\text{FSO}}^{\text{eff}}}^{\mathcal{M}(a)}(\gamma) = \frac{\zeta^2 A}{2} \sum_{m=1}^{\beta} b_m \sum_{l=1}^3 \frac{\prod_{j=1, j \neq l}^3 \Gamma(b'_j - b'_l)}{\Gamma(\zeta^2 + 1 - b'_l) b'_l} \left(\frac{B(\gamma/c)^w}{\mu_s^{1/s}} \right)^{b'_l}, \quad (35)$$

⁸Since by definition, μ_s is proportional to $\bar{\gamma}_{\text{FSO}}$ (see the definitions after (17)).

where $b'_1 = \zeta^2, b'_2 = \alpha$ and $b'_3 = m$. Further, (35) can be reduced more by keeping the dominant term only in the second summation ($\sum_{l=1}^3$) on the high FSO SNR ($\frac{1}{\mu_s} \rightarrow 0$), i.e., the term which has the smallest b'_l ($b'_{\text{min}} \triangleq \min[\zeta^2, \alpha, m]$). This reduction leads to

$$F_{\gamma_{\text{FSO}}^{\text{eff}}}^{\mathcal{M}(a)}(\gamma) = \frac{\zeta^2 A}{2} \sum_{m=1}^{\beta} b_m \frac{\prod_{j=1, b'_j \neq b'_{\text{min}}}^3 \Gamma(b'_j - b'_{\text{min}})}{\Gamma(\zeta^2 + 1 - b'_{\text{min}}) b'_{\text{min}}} \left(\frac{B(\gamma/c)^w}{\mu_s^{1/s}} \right)^{b'_{\text{min}}}. \quad (36)$$

For the case of $\rho \neq 1$, and by using the definition of b'_{min} , Eq. (36) can be represented as

$$F_{\gamma_{\text{FSO}}^{\text{eff}}}^{\mathcal{M}(a)}(\gamma) = \Lambda \left(B(\gamma/c)^w / \mu_s^{1/s} \right)^{b'_{\text{min}}}, \quad (37)$$

where $b''_{\text{min}} = \min[\zeta^2, \alpha, 1]$, and $\Lambda / \frac{\zeta^2 A}{2} \triangleq$

$$\begin{cases} \sum_{m=1}^{\beta} b_m \frac{\prod_{j=1, b'_j \neq b'_{\text{min}}}^3 \Gamma(b'_j - b'_{\text{min}})}{\Gamma(\zeta^2 + 1 - b'_{\text{min}}) b'_{\text{min}}} & \text{if } \zeta^2 \text{ or } \alpha < 1, \Rightarrow b'_{\text{min}} \\ & = \min[\zeta^2, \alpha] \\ b_1 \frac{\Gamma(\zeta^2 - 1) \Gamma(\alpha - 1)}{\Gamma(\zeta^2) \times 1} & \text{if } \zeta^2 \& \alpha > 1, \Rightarrow b'_{\text{min}} = 1 \end{cases},$$

where in case of $b'_{\text{min}} = 1$, we keep only the term which has $m = 1$ in the summation with respect to m , since this is the term which dominates on the high FSO SNRs.

Now by using (34) and (37) in (33), we attain

$$P_{\text{out}}^{(a)} = \left(\frac{(d^2!)^{1/d^2} \bar{\gamma}_{\text{RF}}}{d^2 \gamma_{\text{out1}}} \right)^{-d^2} + \left(\frac{\Lambda^{-s/b''_{\text{min}}} B^{-s} \mu_s}{(\gamma_{\text{out2}}/c)^{ws}} \right)^{-b''_{\text{min}}/s}. \quad (38)$$

For the $P_{\text{out}}^{(a)}$ in (38), let's focus on the following cases:

Case 1: The 1st hop dominates the P_{out} of the system
This is the case whenever the first summand in (38) is much bigger than the second one, i.e., the 1st hop (RF link) is in worse situations than the 2nd hop (FSO link). This case occurs for example if the FSO link meets relatively weak turbulence condition and insignificant pointing errors, i.e., where α, β , and ζ possess relatively high values. Also, this case can occur wherever the MIMO RF link possess relatively low average effective SNR.

By referring to the standard $P_{\text{out}}^{(a)}$ formula, it can be noticed that, in this case, the system under consideration can attain the following diversity order and coding gain, respectively,

$$G_d^{\text{RF}} = d^2, \quad (39a)$$

$$G_c^{\text{RF}} = (d^2!)^{1/d^2} / (d^2 \gamma_{\text{out1}}). \quad (39b)$$

Case 2: The 2nd hop dominates the P_{out} of the system
This is the case whenever the second term in (38) is much greater than the first term, i.e., the 2nd hop (the FSO link) faces worse situations than the 1st hop (the RF link).

⁹The case of $\rho = 1$ (i.e $g = 0$), which leads to $Ab_m = 0$ for all m except $m = \beta$, is considered after (40b).

As an example, this case takes place if the FSO link meets relatively strong turbulent condition and considerable pointing mismatches, i.e., where α , β , and ζ possess relatively smaller values. This case can occur also wherever the MIMO RF link possess relatively big average effective SNR.

Then, by referring to the standard $P_{out}^{(a)}$ formula, it is noticed that, in this case, the achieved diversity order and coding gain of our considered relaying are, respectively,

$$G_d^M = b_{min}''/s = \min[\zeta^2, \alpha, 1]/s, \quad (40a)$$

$$G_c^M = \Lambda^{-s/b_{min}''} B^{-s}/(\gamma_{out2}/c)^{ws}. \quad (40b)$$

The above $P_{out}^{(a)}$ in (38), and so ((40a), (40b)) are wherever the FSO hop faces the M fadings with $\rho \neq 1$. However, to obtain the $P_{out}^{(a)}$ at the special case of the GG fadings ($\rho = 1$) on the FSO hop, the CDF $F_{\gamma_{FSO}^{eff}}^{M(a)}(\gamma)$ in (33) must be exchanged by the CDF $F_{\gamma_{FSO}^{eff}}^{GG(a)}(\gamma)$ which is expressed, after applying $\Omega' = 1$ (for normalization) and $\rho = 1$ in (36), as

$$F_{\gamma_{FSO}^{eff}}^{GG(a)}(\gamma) = \left(\Delta^{1/b_{min}^*} (\gamma/c)^w / \mu_s^{1/s} \right)^{b_{min}^*}, \quad (41)$$

where $b_1^* = \zeta^2$, $b_2^* = \alpha$, $b_3^* = \beta$, $b_{min}^* = \min[\zeta^2, \alpha, \beta]$, and $\Delta \triangleq \frac{\zeta^2}{\Gamma(\alpha)\Gamma(\beta)} \left(\frac{\zeta^2\alpha\beta}{\zeta^2+1} \right)^{b_{min}^*} \frac{\prod_{j=1, b_j^* \neq b_{min}^*}^3 \Gamma(b_j^* - b_{min}^*)}{\Gamma(\zeta^2+1-b_{min}^*)b_{min}^*}$.

Therefore, by exploiting (34) and (41), we attain the $P_{out}^{(a)}$ in case of GG fading on the FSO hop as follows

$$P_{out}^{(a)} = F_{\gamma_{RF}}^{(a)}(\gamma_{out1}) + F_{\gamma_{FSO}^{eff}}^{GG(a)}(\gamma_{out2}) \quad (42)$$

$$= \left(\frac{(d^2)^{1/d^2} \bar{\gamma}_{RF}}{d^2 \gamma_{out1}} \right)^{-d^2} + \left(\frac{\Delta^{-s/b_{min}^*} \mu_s}{(\gamma_{out2}/c)^{ws}} \right)^{-b_{min}^*/s}. \quad (43)$$

Then again for $P_{out}^{(a)}$ in (43), we explore the prior mentioned two cases. In regard to case 1, nothing changes, and thus we can infer the same previous results. Whereas, for case 2, i.e., wherever the 2nd summand is dominant in (43), we can observe that, related to P_{out} , our considered system can attain the following diversity order and coding gain, respectively,

$$G_d^{GG} = b_{min}^*/s = \min[\zeta^2, \alpha, \beta]/s, \quad (44a)$$

$$G_c^{GG} = \Delta^{-s/b_{min}^*} / (\gamma_{out2}/c)^{ws}. \quad (44b)$$

It is important to notice that it is possible for G_d^{GG} to be higher than $1/s$, however this is not possible for G_d^M . Another note is that in the FSO link, G_c is different for each FSO detector. Whereas, based on the previous high SNR analyses, using HD or IMDD cost-dependent leads to the same G_d which is twice the G_d of IMDD input-independent. Nevertheless, if the asymptotic analyses is based on high transmitted power region, all these FSO detectors will lead to the same P_{out} -based diversity order (call it G_{dp}). To elucidate this consider the aforementioned ‘‘case 2’’, and by referring to (38), (43), and remembering that μ_s is proportional to P_r^* (see the definitions after (17)), it can be shown that, for all considered

FSO detectors, we get

$$G_{dp}^M = \min[\zeta^2, \alpha, 1], \quad (45a)$$

$$G_{dp}^{GG} = \min[\zeta^2, \alpha, \beta]. \quad (45b)$$

C. ERGODIC CHANNEL CAPACITY

The ergodic channel capacity (C_{erg}) is the information theoretical channel capacity in the case of the fast fadings channel [34]. As in dualhop DF relaying systems, the ergodic capacity in our considered system¹⁰ is given by

$$C_{erg} = \frac{1}{2} \min \left[\mathbb{E}\{C_{RF}\}, \mathbb{E}\{C_{FSO}\} \right], \quad (46)$$

where C_{RF} and C_{FSO} are presented in (22) and (24), respectively, and hence the above expectations are obtained by

$$\mathbb{E}\{C_{RF}\} = \frac{1}{\ln(2)} \int_0^\infty d \ln(1 + \gamma) f_{\gamma_{RF}}(\gamma) d\gamma. \quad (47)$$

$$\mathbb{E}\{C_{FSO}\} = \frac{1}{\ln(2)} \int_0^\infty \ln(1 + \gamma) f_{\gamma_{FSO}^{eff}}^M(\gamma) d\gamma. \quad (48)$$

Then by substituting (23) in (47), while using $\ln(1 + \gamma) = G_{2,2}^{1,2}[\gamma|_{1,0}^{1,1}]$ and $\exp(-z) = G_{0,1}^{1,0}[z|_0^-]$, and with the helps of [37, Eq. (07.34.21.0013.01), Eq. (07.34.17.0011.01)], we attain

$$\mathbb{E}\{C_{RF}\} = d \frac{(d^2/\bar{\gamma}_{RF})^{d^2}}{(d^2 - 1)! \ln 2} G_{2,3}^{3,1} \left[\frac{d^2}{\bar{\gamma}_{RF}} \middle|_{0, -d^2, -d^2}^{-d^2, 1-d^2} \right]. \quad (49)$$

On the other hand, by substituting (25) in (48) and using $\ln(1 + \gamma) = G_{2,2}^{1,2}[\gamma|_{1,0}^{1,1}]$, $\mathbb{E}\{C_{FSO}\}$ can be obtained by exploiting [37, Eq. (07.34.21.0013.01)]. By doing that, and after some manipulations by utilizing the Meijer’s G-function definition [33, Eq. (9.301)], we get

$$\mathbb{E}\{C_{FSO}\} = \frac{\zeta^2 A/2}{(2\pi)^{w-1} \ln 2} \sum_{m=1}^{\beta} b_m G_{w+2, w+4}^{w+4, w} \left[\frac{B/c^w}{\mu_s^{1/s}} \middle|_{\zeta^2, \alpha, m, 0, \mathbf{x}_1}^{\mathbf{x}_1, 1, \zeta^2+1} \right], \quad (50)$$

where $\mathbf{x}_1 = \frac{0}{w}, \dots, \frac{w-1}{w}$ which has w terms.

Eventually, substituting (49) and (50) in (46) leads to the ergodic capacity of the considered system.

Note that the $\mathbb{E}\{C_{FSO}\}$ in (50) is for the M fadings FSO channel. Alternatively, to attain the $\mathbb{E}\{C_{FSO}\}$ at the special case of GG fadings FSO channel, the pdf $f_{\gamma_{FSO}^{eff}}^M(\gamma)$ in (48) must be changed by the pdf $f_{\gamma_{FSO}^{eff}}^{GG}(\gamma)$ given in (26). By doing that, and following the same steps as the prior ones, we obtain

$$\begin{aligned} \mathbb{E}\{C_{FSO}\} &= \frac{\zeta^2/(\Gamma(\alpha)\Gamma(\beta))}{(2\pi)^{w-1} \ln 2} G_{w+2, w+4}^{w+4, w} \left[\frac{\zeta^2\alpha\beta/c^w}{(\zeta^2 + 1)\mu_s^{1/s}} \middle|_{\zeta^2, \alpha, \beta, 0, \mathbf{x}_1}^{\mathbf{x}_1, 1, \zeta^2+1} \right]. \end{aligned} \quad (51)$$

¹⁰Generally, the RF and FSO fadings channels are slow fadings channels. Nonetheless, they can be seen as fast fadings channels when long enough interleaving is employed especially in some conditions such as in the windy condition when the RF and FSO channels (especially the FSO pointing error) fluctuate in a fast manner.

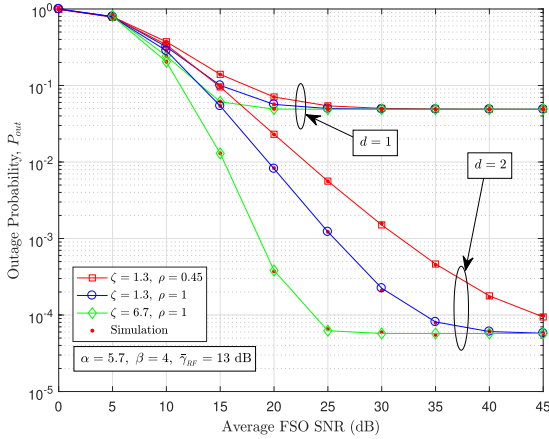


FIGURE 2. P_{out} for different values of the DoF (d), ζ and ρ considering the IMDD cost-dependent FSO.

IV. SIMULATION AND NUMERICAL RESULTS

In this section, we present numerical examples to demonstrate the analytical exact and asymptotic expressions of the previous section and also to illustrate the impact of the various system and channel parameters on the performance of our system.¹¹ Additionally, this section verifies the obtained analytical and asymptotic expressions through Monte-Carlo simulations. In these simulations, 10^6 realizations of the SNR random variable are used.¹²

The effects of various values of the DoF (d), ρ and ζ (the pointing errors) on the system outage probability is shown in Fig. 2 for fixed atmospheric turbulence scenario (α and β) in case of IMDD cost-dependent. From this figure, it can be perceived that the higher values of ρ , d (more DoF), or ζ (smaller pointing mismatches) give lower value of P_{out} , and so better performance is gotten. In addition, according to the used parameters, we can see from this figure that at low average FSO SNRs the P_{out} is dominated by the FSO hop, i.e., P_{out} changes with the change in $\bar{\gamma}_{FSO}$ even though $\bar{\gamma}_{RF}$ is fixed here. Whereas, in this figure at relatively high FSO SNRs the P_{out} is constant since it is dominated by the RF hop for which $\bar{\gamma}_{RF}$ is kept constant in this case. Moreover, Fig. 2 shows that, from power allocation point of view, there is no benefit in increasing $\bar{\gamma}_{FSO}$ when the system outage is dominated by the RF hop, this is specially clear in case of small values of DoF (e.g. $d = 1$).

Fig. 3 illustrates the influences of the atmospheric turbulence parameters (α and β) on P_{out} for a fixed pointing errors ($\zeta = 2$). It can be clearly seen that the smaller values of α and β , i.e., tougher atmospheric turbulences, give bigger (worse) P_{out} and the higher values of α and β result in lower outage probability. Beside that, we can perceive from Fig. 3 that at lower average RF SNRs the RF link

¹¹Following the same approach as in the related literature, e.g. [11], [17], [30], [31], the values of the system parameters were chosen to confirm the deduced expressions, and thence other parameters values can be used by the designer to attain the needed result in specific schemes.

¹²In these results, without loss of generality, we set $\Omega = 0.78$ and $b_0 = 0.11$.

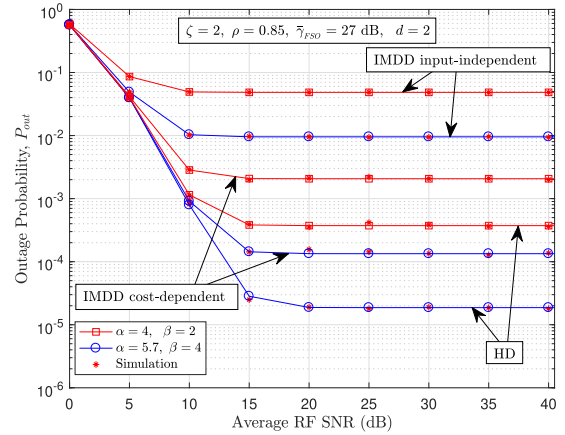


FIGURE 3. P_{out} for various values of α and β considering all FSO detection methods.

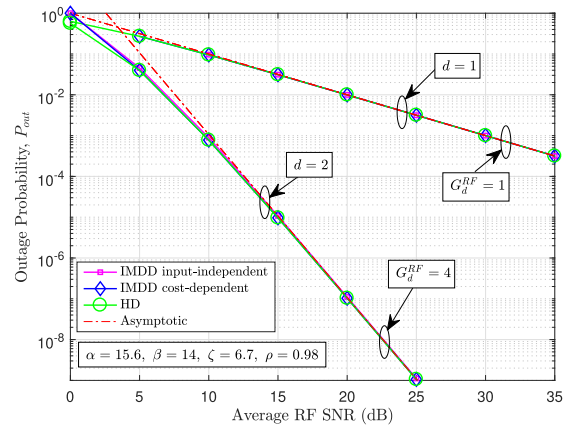


FIGURE 4. P_{out} dominated by the RF hop with different DoF(d) considering all FSO detection techniques.

dominates our P_{out} , i.e., P_{out} changes when $\bar{\gamma}_{RF}$ varies though $\bar{\gamma}_{FSO}$ is set constant in this figure. Whereas, as seen from this figure at relatively high RF SNRs the P_{out} becomes constant, as it is dominated by the FSO link for which $\bar{\gamma}_{FSO}$ is kept fixed in this case. Then again, from power allocation point of view there is no benefit in increasing $\bar{\gamma}_{RF}$ when the FSO channel dominates the system outage as seen from Fig. 3. This is particularly clear in the case of the IMDD input-independent.

Fig. 4 and Fig. 5 prove that the asymptotic expression of P_{out} converges to the exact P_{out} expression in the high SNR region. Moreover, these figures explain the coding gain and diversity order of the system outage probability in the high SNR for various cases. Particularly, Fig. 4 evinces that $G_d^{RF} = d^2$ as derived before in Section III-B, i.e., the measured slopes of the log-log curves at high SNRs in Fig. 4 equal the derived G_d^{RF} .

On the other hand, Fig. 5 validates that, given $s = 1$, $G_d^M = b''_{min}/s = \min[\zeta^2, \alpha, 1]$ and $G_d^{GG} = b^*_{min}/s = \min[\zeta^2, \alpha, \beta]$ as drawn previously in Section III-B, i.e., on the high SNR region in Fig. 5 the labeled measured log-log slopes are identical to the former derived ones.

Fig. 6 relates the ergodic channel capacity (C_{erg}) in the y axis with the average RF SNR ($\bar{\gamma}_{RF}$) in the x axis for different

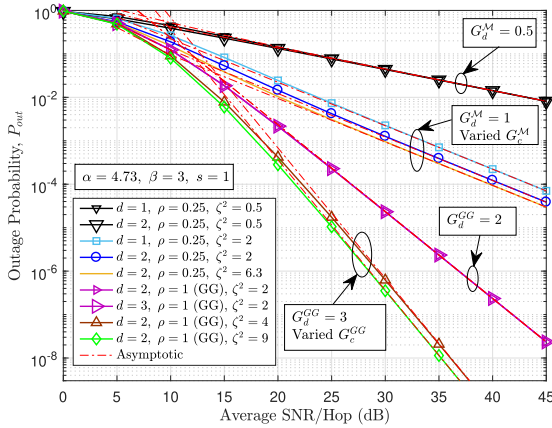


FIGURE 5. P_{out} dominated by FSO IMDD cost-dependent hop with different values of the DoF (d), ρ and ζ .

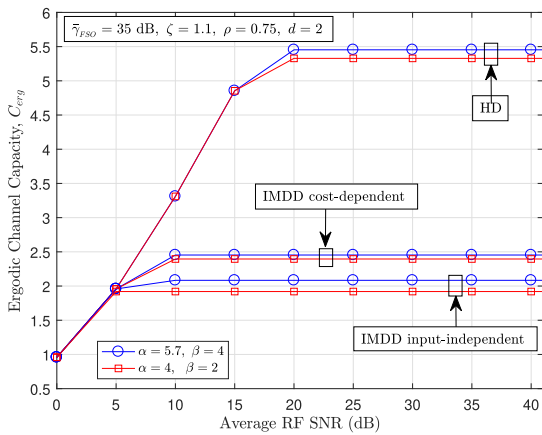


FIGURE 6. C_{erg} for various values of α and β considering all FSO detection methods.

values of the atmospheric turbulence parameters (α and β), when the pointing error (ζ), the average FSO SNR ($\bar{\gamma}_{FSO}$) and the DoF (d) are kept constant. It can be seen that, stronger atmospheric turbulence, i.e., lower values of α and β , gives lower (worse) C_{erg} and higher values of α and β result in higher C_{erg} . In addition, based on the used parameters, we can also note that in the relatively low RF SNRs region the RF hop dominates the C_{erg} , i.e., C_{erg} varies with the changes in $\bar{\gamma}_{RF}$ though $\bar{\gamma}_{FSO}$ is set constant here. Whereas, C_{erg} will be constant, if the RF SNR is relatively high, because it will be dominated in this case by the FSO hop for which $\bar{\gamma}_{FSO}$ is set constant.

The impact of the number of the interference-eliminated RF info streams (d) on the system ergodic channel capacity (C_{erg}) is provided in Fig. 7 for all considered FSO detectors. It can be observed that the overall system ergodic capacity enhances by increasing d when the RF hop dominates the C_{erg} (i.e. at relatively low RF SNRs). We can also see from this figure that the capacity pre-log (DoF) equals d in the RF domination region. Moreover, it is clear from Fig. 7 that increasing $\bar{\gamma}_{RF}$ or d will not improve the C_{erg} in the FSO domination region (i.e. at relatively high RF SNRs and specially when IMDD is used). Further, Fig. 7 reflects that there is no benefit in changing the FSO detector when C_{erg} is

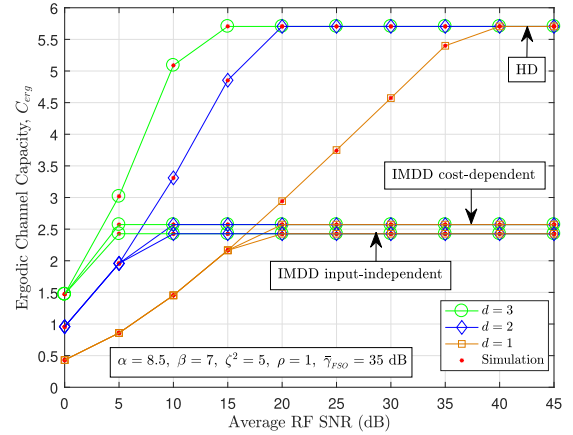


FIGURE 7. C_{erg} for different DoF (d) in the RF hop considering all FSO detection methods in the FSO hop.

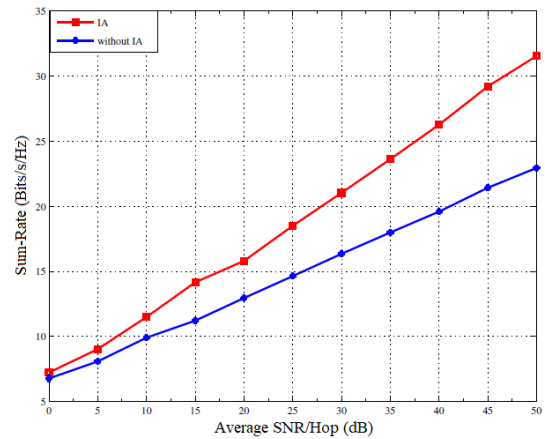


FIGURE 8. User-Sum rate in mixed MIMO RF IC/FSO cellular network.

dominated by the RF hop (i.e. at relatively low RF SNRs and specially with $d = 1$).

In Fig. 8, the user-sum rate in the mixed interference aligned RF/FSO cellular network is simulated using (12) and (13), and compared with traditional orthogonal multiple access (e.g. TDMA) mixed RF/FSO cellular network. Since the IA technique enables all users from utilizing the total bandwidth simultaneously, therefore using this technique in the mixed RF/FSO improves the user-sum rate as shown in Fig.8.

V. CONCLUSION

This paper studied a dual-hop DF mixed (MIMO RF IC)/ (FSO) relaying scheme in which HD as well as IMDD were considered in a unified manner in the FSO hop. It was assumed that the MIMO RF links follow Rayleigh fading, while the FSO link suffers \mathcal{M} fading with pointing errors. In the MIMO RF IC hop, the IA technique was utilized to eliminate the interference, and hence this leads to enhance the multiplexing gain in this hop, and accordingly the overall system performance is improved. The IA precoding and receiving interference eliminating matrices were designed by using adapting OR-ML algorithm. For this scheme, closed-form

expressions were derived for the outage probability and ergodic capacity, in these expressions the best-known FSO channel capacity results were utilized. Moreover, not only the IMDD input-independent AWGN but also the IMDD cost-dependent AWGN channel was analyzed in these investigations. Additionally, the system performance was asymptotically studied on the high SNRs region, where the diversity order and coding gain analyses were illustrated. It was found that under RF hop domination, the diversity order equals the square of the number of the interference-eliminated RF info streams (d^2). Alternatively, under FSO hop domination, the diversity order depends on the parameters of the atmospheric turbulences and pointing errors. Also, It was observed that the overall system ergodic capacity enhances by increasing d when the RF hop dominates the system. Further, we provided simulation results that verify the deduced analytical and asymptotic expressions.

REFERENCES

- [1] S. Arnon, J. Barry, G. Karagiannidis, R. Schober, and M. Uysal, *Advanced Optical Wireless Communication Systems*. Cambridge, U.K.: Cambridge Univ. Press, 2012.
- [2] M. A. Khalighi and M. Uysal, "Survey on free space optical communication: A communication theory perspective," *IEEE Commun. Surveys Tuts.*, vol. 16, no. 4, pp. 2231–2258, 4th Quart., 2014.
- [3] V. Jamali, D. S. Michalopoulos, M. Uysal, and R. Schober, "Mixed RF and hybrid RF/FSO relaying," in *Proc. IEEE Globecom Workshops (GC Wkshps)*, San Diego, CA, USA, Dec. 2015, pp. 1–6.
- [4] I. S. Ansari, F. Yilmaz, and M.-S. Alouini, "On the performance of mixed RF/FSO variable gain dual-hop transmission systems with pointing errors," in *Proc. IEEE 78th Veh. Technol. Conf. (VTC Fall)*, Las Vegas, NV, USA, Sep. 2013, pp. 1–5.
- [5] M. R. Bhatnagar and M. K. Arti, "Performance analysis of hybrid satellite-terrestrial FSO cooperative system," *IEEE Photon. Technol. Lett.*, vol. 25, no. 22, pp. 2197–2200, Nov. 2013.
- [6] H. Samimi and M. Uysal, "End-to-end performance of mixed RF/FSO transmission systems," *J. Opt. Commun. Netw.*, vol. 5, no. 11, pp. 1139–1144, Nov. 2013.
- [7] I. S. Ansari, M.-S. Alouini, and F. Yilmaz, "On the performance of hybrid RF and RF/FSO fixed gain dual-hop transmission systems," in *Proc. Saudi Int. Electron., Commun. Photon. Conf.*, Riyadh, Saudi Arabia, Apr. 2013, pp. 1–6.
- [8] S. Anees and M. R. Bhatnagar, "Performance of an amplify-and-forward dual-hop asymmetric RF-FSO communication system," *J. Opt. Commun. Netw.*, vol. 7, no. 2, pp. 124–135, Feb. 2015.
- [9] E. Zedini, I. S. Ansari, and M.-S. Alouini, "On the performance of hybrid line of sight RF and RF-FSO fixed gain dual-hop transmission systems," in *Proc. IEEE Global Commun. Conf.*, Dec. 2014, pp. 2119–2124.
- [10] E. Zedini, I. S. Ansari, and M.-S. Alouini, "Performance analysis of mixed Nakagami- m and Gamma-Gamma dual-hop FSO transmission systems," *IEEE Photon. J.*, vol. 7, no. 1, pp. 1–20, Feb. 2015.
- [11] A. M. Salhab, F. S. Al-Qahtani, R. M. Radaydeh, S. A. Zummo, and H. Alnuweiri, "Power allocation and performance of multiuser mixed RF/FSO relay networks with opportunistic scheduling and outdated channel information," *J. Lightw. Technol.*, vol. 34, no. 13, pp. 3259–3272, Jul. 1, 2016.
- [12] A. M. Salhab, "Performance of multiuser mixed RF/FSO relay networks with generalized order user scheduling and outdated channel information," *Arabian J. for Sci. Eng.*, vol. 40, no. 9, pp. 2671–2683, Sep. 2015.
- [13] E. Soleimani-Nasab and M. Uysal, "Generalized performance analysis of mixed RF/FSO cooperative systems," *IEEE Trans. Wireless Commun.*, vol. 15, no. 1, pp. 714–727, Jan. 2016.
- [14] O. M. S. Al-Ebraheemy, A. M. Salhab, A. Chaaban, S. A. Zummo, and M.-S. Alouini, "Precise performance analysis of dual-hop mixed RF/Unified-FSO DF relaying with heterodyne detection and two IM-DD channel models," *IEEE Photon. J.*, vol. 11, no. 1, pp. 1–22, Feb. 2019.
- [15] Y. F. Al-Eryani, A. M. Salhab, S. A. Zummo, and M.-S. Alouini, "Two-way multiuser mixed RF/FSO relaying: Performance analysis and power allocation," *J. Opt. Commun. Netw.*, vol. 10, no. 4, pp. 396–408, Apr. 2018.
- [16] N. Varshney and A. K. Jagannatham, "Cognitive decode-and-forward MIMO-RF/FSO cooperative relay networks," *IEEE Commun. Lett.*, vol. 21, no. 4, pp. 893–896, Apr. 2017.
- [17] N. I. Miridakis, M. Matthaiou, and G. K. Karagiannidis, "Multiuser relaying over mixed RF/FSO links," *IEEE Trans. Commun.*, vol. 62, no. 5, pp. 1634–1645, May 2014.
- [18] N. Sharma, P. Garg, and A. Bansal, "Decode-and-forward relaying in mixed $\eta - \mu$ and gamma-gamma dual hop transmission system," *IET Commun.*, vol. 10, no. 14, pp. 1769–1776, Sep. 2016.
- [19] C. E. Shannon, "A mathematical theory of communication," *Bell Syst. Tech. J.*, vol. 27, no. 3, pp. 379–423, Jul./Oct. 1948.
- [20] O. M. S. Al-Ebraheemy, A. M. Salhab, A. Chaaban, S. A. Zummo, and M.-S. Alouini, "Precise outage analysis of mixed RF/unified-FSO DF relaying with HD and 2 IM-DD channel models," in *Proc. 13th Int. Wireless Commun. Mobile Comput. Conf. (IWCMC)*, Valencia, Spain, Jun. 2017, pp. 1184–1189.
- [21] A. Lapidoth, S. M. Moser, and M. A. Wigger, "On the capacity of free-space optical intensity channels," *IEEE Trans. Inf. Theory*, vol. 55, no. 10, pp. 4449–4461, Oct. 2009.
- [22] A. Chaaban, J.-M. Morvan, and M.-S. Alouini, "Free-space optical communications: Capacity bounds, approximations, and a new sphere-packing perspective," *IEEE Trans. Commun.*, vol. 64, no. 3, pp. 1176–1191, Mar. 2016.
- [23] A. Chaaban and M. S. Alouini, "Optical intensity modulation direct detection versus heterodyne detection: A high-SNR capacity comparison," in *Proc. 5th Int. Conf. Commun. Netw. (COMNET)*, Tunis, Tunisia, Nov. 2015, pp. 1–5.
- [24] A. Chaaban, J. M. Morvan, and M.-S. Alouini, "Free-space optical communications: Capacity bounds, approximations, and a new sphere-packing perspective," Kaust, Thuwal, Saudi Arabia, Tech. Rep., Apr. 2015. [Online]. Available: <http://hdl.handle.net/10754/552096>
- [25] A. H. A. El-Malek, A. M. Salhab, S. A. Zummo, and M.-S. Alouini, "Effect of RF interference on the security-reliability tradeoff analysis of multiuser mixed RF/FSO relay networks with power allocation," *J. Lightw. Technol.*, vol. 35, no. 9, pp. 1490–1505, May 1, 2017.
- [26] A. B. Carleial, "Interference channels," *IEEE Trans. Inf. Theory*, vol. 24, no. 1, pp. 60–70, Jan. 1978.
- [27] V. R. Cadambe and S. A. Jafar, "Interference alignment and the degrees of freedom for the K-user interference channel," *IEEE Trans. Info. Theory*, vol. 54, no. 8, pp. 3425–3441, Aug. 2008.
- [28] C. M. Yetis, T. Gou, S. A. Jafar, and A. H. Kayran, "On feasibility of interference alignment in MIMO interference networks," *IEEE Trans. Signal Process.*, vol. 58, no. 9, pp. 4771–4782, Sep. 2010.
- [29] M. K. Simon and M.-S. Alouini, *Digital Communication Over Fading Channels*, 2nd ed. Hoboken, NJ, USA: Wiley, 2005.
- [30] A. J. Navas, J. M. G. Balsells, J. F. Paris, and A. P. Notario, "A unifying statistical model for atmospheric optical scintillation," in *Numerical Simulations of Physical and Engineering Processes*, J. Awrejcewicz, Ed. Rijeka, Croatia: InTech, 2011, ch. 8.
- [31] A. Jurado-Navas, J. M. Garrido-Balsells, J. F. Paris, M. Castillo-Vázquez, and A. Puerta-Notario, "Impact of pointing errors on the performance of generalized atmospheric optical channels," *Opt. Express*, vol. 20, no. 11, pp. 12550–12562, May 2012.
- [32] A. A. Farid and S. Hranilovic, "Outage capacity optimization for free-space optical links with pointing errors," *J. Lightw. Technol.*, vol. 25, no. 7, pp. 1702–1710, Jul. 2007.
- [33] I. S. Gradshteyn and I. M. Ryzhik, *Table of Integrals, Series, and Products*, 6th ed. San Diego, CA, USA: Academic, 2000.
- [34] D. Tse and P. Viswanath, *Fundamentals of Wireless Communication*. Cambridge, U.K.: Cambridge Univ. Press, 2005.
- [35] J. G. Proakis and M. Salehi, *Digital Communications*. New York, NY, USA: McGraw-Hill, 2008.
- [36] A. Papoulis and S. U. Pillai, *Probability, Random Variables, and Stochastic Processes*. New York, NY, USA: McGraw-Hill, 2002.
- [37] Wolfram. (2019). *The Wolfram Functions Site*. [Online]. Available: <http://functions.wolfram.com>

OMER MAHMOUD SALIH AL-EBRAHEEMY received the B.Sc. degree in electrical engineering from the University of Khartoum, Khartoum, Sudan, in 2004, the M.Sc. degree in electrical engineering from the Blekinge Institute of Technology, Blekinge, Sweden, in 2012, and the Ph.D. degree in electrical engineering from the King Fahd University of Petroleum and Minerals (KFUPM), Dhahran, Saudi Arabia, in 2019. He has over five years of experience with wireless cellular network operators and system vendors in 2G and 3G radio network planning and optimization. His research interests include signal processing, information theory, and wireless communications. He was a recipient of the Best Academic Performance Award from the Faculty of Engineering, University of Khartoum, the ZAIN Aim for Excellence Award for exceptional performance in developing the DDS feature in their cellular network, in 2009, and the Ph.D. Scholarship from KFUPM, in 2013.

ANAS M. SALHAB (Senior Member, IEEE) received the B.Sc. degree in electrical engineering from Palestine Polytechnic University, Hebron, Palestine, in 2004, the M.Sc. degree in electrical engineering from the Jordan University of Science and Technology, Irbid, Jordan, in 2007, and the Ph.D. degree from the King Fahd University of Petroleum and Minerals (KFUPM), Dhahran, Saudi Arabia, in 2013. From 2013 to 2014, he was a Postdoctoral Fellow with the Electrical Engineering Department, KFUPM. He is currently an Assistant Professor and the Assistant Director of the Science and Technology Unit with the Deanship of Scientific Research, KFUPM. His research interest spans special topics in modeling and performance analysis of wireless communication systems, including cooperative relay networks, cognitive radio relay networks, free space optical networks, visible light communications, and co-channel interference. He was selected as an Exemplary Reviewer by the IEEE WIRELESS COMMUNICATIONS LETTERS for his reviewing service, in 2014. Also, he received the KFUPM Best Research Project Award as a Co-Investigator among the projects in 2013/2014 and 2014/2015.

MOHAMMED EL-ABSI received the B.E. degree in electrical engineering from the Islamic University of Gaza, Gaza, Palestine, in 2005, the M.S. degree in electrical engineering from the Jordan University of Science and Technology, in 2008, and the Ph.D. degree (*summa cum laude*) in electrical engineering from the University of Duisburg-Essen, Duisburg, Germany, in 2015. He is currently working as a Senior Researcher with the Collaborative Research Center “Mobile Material Characterization and Localization by Electromagnetic Sensing” (MARIE) project, Digital Signal Processing Institute, University of Duisburg-Essen. His research interests are in the area of communications and signal processing. He received the German Academic Exchange Service Fellowship, in 2006 and 2011.

SALAM A. ZUMMO (Senior Member, IEEE) received the B.Sc. and M.Sc. degrees in electrical engineering from the King Fahd University of Petroleum and Minerals (KFUPM), Dhahran, Saudi Arabia, in 1998 and 1999, respectively, and the Ph.D. degree from the University of Michigan, Ann Arbor, USA, in 2003. He is currently a Professor with the Electrical Engineering Department, KFUPM. He has six issued U.S. patents and authored over 100 articles in reputable journals and conference proceedings. His research interests are in the area of wireless communications, including cooperative diversity, cognitive radio, multiuser diversity, scheduling, MIMO systems, error control coding, multihop networks, and interference modeling and analysis in wireless systems. He received the Saudi Ambassador Award for early Ph.D. completion, in 2003, and the British Council/BAE Research Fellowship Awards, in 2004 and 2006. He also received the KFUPM Excellence in Research Award, from 2011 to 2012.

SALAMA S. IKKI (Senior Member, IEEE) received the B.S. degree from Al-Isra University, Amman, Jordan, in 1996, the M.Sc. degree from The Arab Academy for Science and Technology and Maritime Transport, Alexandria, Egypt, in 2002, and the Ph.D. degree from Memorial University, St. Johns, NL, Canada, in 2009, all in electrical engineering. From February 2009 to February 2010, he was a Postdoctoral Researcher with the University of Waterloo, ON, Canada. From February 2010 to December 2012, he was a Research Assistant with INRS, University of Quebec, Montreal, QC, Canada. He is currently an Associate Professor of wireless communications with Lakehead University, Thunder Bay, ON. He is the author of 120 journals and conference papers and has more than 3200 citations and an H-index of 30. His research interests include cooperative networks, multiple-input-multiple-output, spatial modulation, and wireless sensor networks. He has served as a Technical Program Committee member for various conferences, including the IEEE International Conference on Communications, the IEEE Global Communications Conference, the IEEE Wireless Communications and Networking Conference, the IEEE Spring/Fall Vehicular Technology Conference, and the IEEE International Symposium on Personal, Indoor, and Mobile Communications. He currently serves on the Editorial Board of the IEEE COMMUNICATIONS LETTERS and Institution of Engineering and Technology Communications. He received a Best Paper Award for his article published in *EURASIP Journal on Advanced Signal Processing*. He also received an the IEEE COMMUNICATIONS LETTERS, the IEEE WIRELESS COMMUNICATIONS LETTERS and the IEEE TRANSACTIONS ON VEHICULAR TECHNOLOGY exemplary reviewer certificates for 2012, 2012, and 2014, respectively.

• • •